Mineralogical Magazine, August 2018, Vol. 82(4), pp. 809–819

The hydrocerussite-related phase, $NaPb_5(CO_3)_4(OH)_3$, from the ancient slags of Lavrion, Greece

Oleg I. Siidra[1,2,*], Diana O. Nekrasova[1], Nikita V. Chukanov[3], Igor V. Pekov[4], Vasiliy O. Yapaskurt[4], Athanassios Katerinopoulos[5], Panagiotis Voudouris[5], Andreas Magganas[5] and Anatoly N. Zaitsev[6]

[1] Department of Crystallography, St. Petersburg State University, University Embankment 7/9, 199034 St. Petersburg, Russia
[2] Nanomaterials Research Center, Kola Science Center, Russian Academy of Sciences, Apatity, Murmansk Region, 184200, Russia
[3] Institute of Problems of Chemical Physics, Chernogolovka, Moscow Region, 142432, Russia
[4] Faculty of Geology, Moscow State University, Vorobievy Gory, 119991, Moscow, Russia
[5] Department of Mineralogy and Petrology, Faculty of Geology and Geoenvironment, National and Kapodistrian University of Athens, Panepistimioupolis 15784 Athens, Greece
[6] Department of Mineralogy, St. Petersburg State University, University Embankment 7/9, 199034 St. Petersburg, Russia

[*Received 18 April 2017; Accepted 4 July 2017; Associate Editor: Stuart Mills*]

ABSTRACT

The hydrocerussite-related phase, $NaPb_5(CO_3)_4(OH)_3$, has been found as colourless lamellar crystals in cavities within a pebble of the ancient marine slag collected in the Pacha Limani area of the Lavrion mining district, Attiki, Greece. This phase of anthropogenic origin was characterized by electron microprobe, infrared spectroscopy, powder and single-crystal X-ray diffraction. The unique crystal structure ($P6_3/mmc$, $a = 5.2533(11)$, $c = 29.425(6)$ Å, $V = 703.3(3)$ Å^3 and $R_1 = 0.047$) is based upon structurally and chemically different electroneutral blocks. Each of the blocks can be split into separate sheets. The outer sheets in each block are topologically identical and have the composition $[PbCO_3]^0$. The $[Pb(OH)_2]^0$ lead hydroxide sheet is sandwiched between the two $[PbCO_3]^0$ sheets resulting in the formation of the first block $[Pb_3(OH)_2(CO_3)_2]^0$ structurally and compositionally identical to that one in hydrocerussite $Pb_3(OH)_2(CO_3)_2$. Similarly the $[Na(OH)]^0$ sheet is sandwiched between another two $[PbCO_3]^0$ sheets thus forming the $[NaPb_2(OH)(CO_3)_2]^0$ block described previously in the structure of abellaite $NaPb_2(OH)(CO_3)_2$. Stereochemically active lone electron pairs on Pb^{2+} cations are located between the blocks. There are two blocks of each type per unit cell, which corresponds to the following formula: $[Pb_3(OH)_2(CO_3)_2][NaPb_2(OH)(CO_3)_2]$ or $NaPb_5(CO_3)_4(OH)_3$ in the simplified representation. The formation of $NaPb_5(CO_3)_4(OH)_3$ in Lavrion slags is by the contact of lead-rich slags with the sea water over the last two thousand years.

Keywords: hydrocerussite, lead, carbonate, crystal structure, layered structure, lone electron pair, abellaite, Lavrion ancient slags, anthropogenic mineralization.

Introduction

The slags from the famous Lavrion ancient silver and lead mines in Attiki, Greece, were dumped after smelting into the sea where their components have been reacting with the sea water for more than two thousand years, forming various mineral phases including many rare and endemic species (Gelaude *et al*., 1996; Kolitsch *et al*., 2014). All the phases formed in the slags are not currently considered as minerals by the International Mineralogical Association because of their anthropogenic (or 'semi-anthropogenic') origin (Nickel and Grice, 1998).

Hydrocerussite $Pb_3(OH)_2(CO_3)_2$ is a rather common mineral found in more than a hundred

*E-mail: o.siidra@spbu.ru
https://doi.org/10.1180/minmag.2017.081.058

Copyright © Mineralogical Society of Great Britain and Ireland 2018

https://doi.org/10.1180/minmag.2017.081.058 Published online by Cambridge University Press

different locations all over the world (https://www.mindat.org/). Structural information for a powder synthetic material was obtained by Martinetto *et al.* (2002) and crystal structure of hydrocerussite from Merehead quarry, Great Britain was reported very recently by Siidra *et al.*, (2018*a*). Hydrocerussite from the Lavrion slags has been well known for a long time. Unit-cell parameters ($a = 5.24–5.25$ Å and $c = 29.38–29.50$ Å) were determined for the lamellar crystals which are visually similar to hydrocerussite (Kokkoros and Vassiliadis, 1953; Kolitsch *et al.*, 2014). Both of the previous works identified this phase as 'hydrocerussite- or plumbonacrite-related' but different from 'classic' hydrocerussite. According to Kokkoros and Vassiliadis (1953), this non-classic phase is much more common than hydrocerussite in the Pb-rich slags of Lavrion. However its crystal structure has also not been solved. A slag phase with the unit-cell parameters identical to those of abellaite $NaPb_2(OH)(CO_3)_2$ (Ibáñez-Insa *et al.*, 2017) is also rather common in Lavrion slags (Kolitsch *et al.* 2014).

Herein, we report data on $NaPb_5(CO_3)_4(OH)_3$, a hydrocerussite-related lead hydroxycarbonate from Lavrion ancient slags, with a surprisingly complex crystal structure based upon structurally and chemically different electroneutral blocks.

Occurrence

The $NaPb_5(CO_3)_4(OH)_3$ phase described in this paper forms aqua-transparent, colourless lamellar crystals up to 0.01 mm × 0.3 mm × 0.3 mm (similar to that shown in Fig. 1) in cavities within a pebble of ancient marine slag collected in the Pacha Limani area of the Lavrion mining district (37° 40'36''N, 24°3'6''E). It is associated with aragonite and lead. The hydrocerussite-related phase was formed during the 2500 y period that the slag was exposed to seawater, causing reactions with the Pb-rich material in the slag.

Chemical composition

The chemical composition of the $NaPb_5(CO_3)_4(OH)_3$ phase was studied using a Jeol JSM-6480LV scanning electron microscope equipped with an INCA-Wave 500 wavelength-dispersive spectrometer (Laboratory of Analytical Techniques of High Spatial Resolution of Faculty of Geology, Lomonosov Moscow State University), with an acceleration voltage of 20 kV, a beam current of 10 nA, and a 5 μm beam diameter. The following

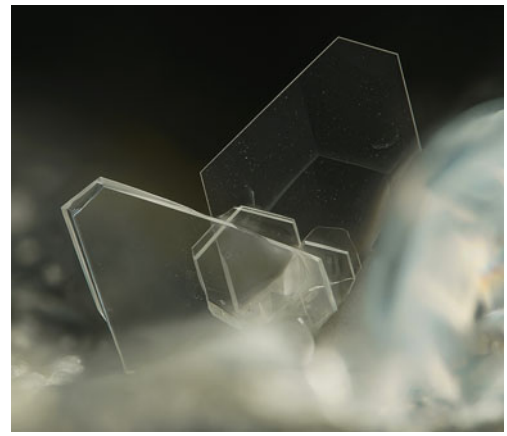

FIG. 1. Typical lamellar transparent colourless crystals of the Na,Ca-bearing hydrocerussite-related phase from Pacha Limani, Lavrion, Greece. Field of view width is 0.6 mm. Photo and collection: S. Wolfsried.

standards were used: NaCl (Na), clinopyroxene (Ca) and PbTe (Pb). Contents of other elements with atomic numbers higher than oxygen are below detection limits. The chemical composition of the phase studied is: Na 0.89, Ca 1.44, Pb 78.05, C_{calc} 3.61, O_{calc} 18.04, H_{calc} 0.19, total 102.22 wt.%. Contents of light elements (C, O and H) were calculated by the stoichiometry for the empirical formula calculated on the basis of Pb + Na + Ca = 6 atoms per formula unit, in accordance with the structural data (see below): $Na_{0.51}Ca_{0.48}Pb_{5.01}(CO_3)_4(OH_{2.51}O_{0.49})_{\Sigma 3}$.

Powder X-ray diffraction data

Powder X-ray diffraction (XRD) data were obtained using a Rigaku R-AXIS Rapid II single-crystal diffractometer equipped with cylindrical image plate detector using Debye-Scherrer geometry (with $d = 127.4$ mm), after crushing the crystal fragments used for the single-crystal XRD analysis. Data (in Å for Co$K\alpha$) are given in Table 1. The unit-cell parameters calculated for a hexagonal unit cell, space group $P6_3/mmc$, are: $a = 5.2514(7)$, $c = 29.428(6)$ Å, $V = 702.8(2)$ Å^3 and $Z = 2$.

Infrared spectroscopy

In order to obtain infrared (IR) absorption spectra, powdered samples of the phase $NaPb_5(CO_3)_4(OH)_3$ from Lavrion and hydrocerussite from Merehead

https://doi.org/10.1180/minmag.2017.081.058 Published online by Cambridge University Press

TABLE 1. Powder X-ray diffraction data for $NaPb_5(CO_3)_4(OH)_3$ from Lavrion.

	Calculated		Measured	
h k l	*d*, Å	*I*, %	*d*, Å	*I*, %
0 0 4	7.356	9	7.354	4
0 0 6	4.904	2	4.905	2
1 0 0	**4.549**	**17**	**4.547**	**13**
1 0 1	4.496	10	4.492	8
1 0 2	4.346	8	4.345	8
1 0 3	**4.127**	**28**	**4.126**	**29**
1 0 4	3.869	7	3.870	7
0 0 8	3.678	2	3.677	3
1 0 5	3.599	1	3.602	2
1 0 6	**3.335**	**100**	**3.336**	**100**
1 0 7	**3.087**	**16**	**3.088**	**18**
0 0 10	**2.942**	**11**	**2.945**	**14**
1 0 8	2.860	2	2.862	3
1 0 9	2.655	2	2.654	2
1 1 0	**2.627**	**46**	**2.626**	**30**
1 1 4	2.474	4	2.473	7
0 0 12	**2.452**	**13**	**2.454**	**17**
2 0 1	2.268	4	2.268	6
2 0 2	2.248	9	2.247	12
2 0 3	2.216	9	2.215	12
1 0 12	2.159	8	2.159	8
0 0 14	2.102	1	2.102	1
2 0 6	**2.064**	**23**	**2.063**	**20**
1 0 13	2.027	6	2.028	6
2 0 7	2.001	5	2.001	5
1 1 10	1.960	3	1.960	4
2 0 8	1.935	4	1.935	4
2 0 9	1.867	3	1.867	2
1 1 12	1.792	7.55	1.792	9

The eight strongest lines are given in bold.

quarry, Somerset, England (Fig. 2), were mixed with anhydrous KBr, pelletized, and analysed using an ALPHA FTIR spectrometer (Bruker Optics) at a resolution of 4 cm^{-1} and 16 scans were collected for each spectrum. The IR spectrum of an analogous pellet of pure KBr was used as a reference.

The IR spectrum of $NaPb_5(CO_3)_4(OH)_3$ contains two bands of O–H-stretching vibrations of OH groups located at 3529 and 3515 cm^{-1}. These values are intermediate between those of hydrocerussite and abellaite, which corresponds to intermediate strengths of H bonds (Libowitzky, 1999). The weak peak at 1735 cm^{-1} is a combination band of the stretching and bending vibrations of CO_3^{2-} groups. The strong band at 1431 cm^{-1} with the shoulder at 1365 cm^{-1} corresponds to the asymmetric stretching vibrations of carbonate groups. The presence of the weak band of symmetric stretching vibrations of carbonate groups at 1044 cm^{-1} (non-degenerate mode) reflects weak distortion of the CO_3 triangle. The bands at 848 and 834 cm^{-1} are assigned to the in-plane bending vibrations of CO_3^{2-} groups. The band at 683 cm^{-1} corresponds to the out-of-plane bending vibrations of CO_3^{2-}. The absorptions below 500 cm^{-1} are the lattice modes involving Pb–O and Na–O stretching and CO_3 librational vibrations.

As can be seen from Fig. 2, the IR spectrum of $NaPb_5(CO_3)_4(OH)_3$ is close to that of abellaite in the region of asymmetric stretching vibrations of carbonate groups and similar to the IR spectrum of hydrocerussite in the region of O–C–O bending vibrations.

Crystal structure

Experiment

The single-crystal study of lead hydroxycarbonate compounds is challenging because of the lamellar habit of crystals, high X-ray absorption and strong pseudosymmetry. Thus, the choice of crystal for XRD study is important. In this work, we have used several thin platy crystals of $NaPb_5(CO_3)_4(OH)_3$. Only the crystals giving the best results are reported below. Crystals of the title compound were mounted on thin glass fibres and placed on a Bruker DUO APEX II CCD four-circle diffractometer with a Mo-IμS micro-focus tube at 50 kV and 40 mA. More than a hemisphere of XRD data was collected with frame widths of 0.5° in ω, and with 90 s counting time for each frame. The data were integrated and corrected for absorption using an empirical ellipsoidal model using the *APEX* and *XPREP* Bruker programs. The observed systematic absences for $NaPb_5(CO_3)_4(OH)_3$ were consistent with the space group $P\bar{3}1c$. In this space group, light atoms (C and O) could not be refined anisotropically. The obtained structure model was transformed to the space group $P6_3/mmc$ using the *ADDSYM* algorithm incorporated in the *PLATON* program package (le Page, 1987; Spek, 2003). The structure was refined successfully with the use of the SHELX software package (Sheldrick, 2015). Structure refinement in this group resulted in the crystallographic agreement index $R_1 = 0.047$ (Table 2). The final coordinates and anisotropic displacement parameters of atoms are given in Table 3 and selected interatomic distances in

https://doi.org/10.1180/minmag.2017.081.058 Published online by Cambridge University Press

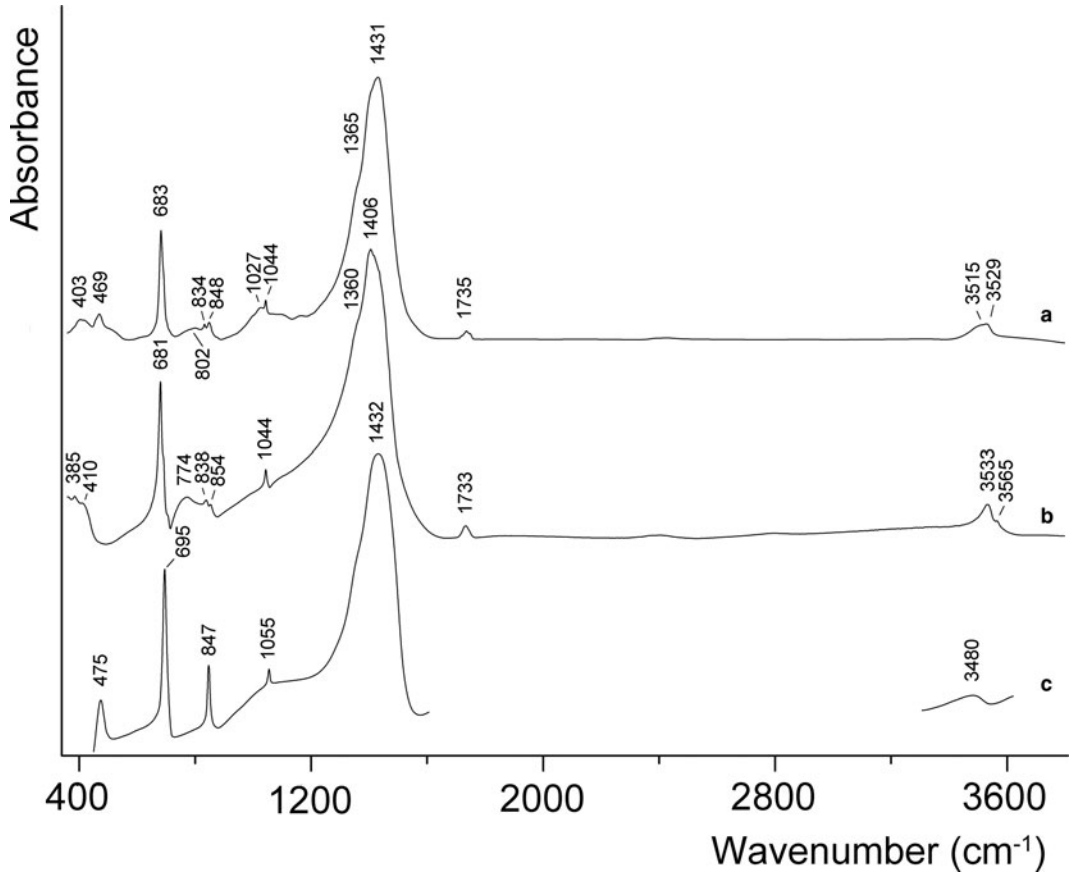

FIG. 2. IR spectra of $NaPb_5(CO_3)_4(OH)_3$ from Lavrion (*a*) and hydrocerussite from the Merehead quarry, Somerset, England (*b*). IR spectrum of synthetic abellaite analogue (*c*) drawn based on data of Belokoneva *et al*. (2002).

Table 4. Hydrogen atom positions were not localized. The crystallographic information files have been deposited with the Principal Editor of *Mineralogical Magazine* and are available as Supplementary material (see below).

Cation and anion coordination

The structure contains three symmetrically independent Pb sites, one Na site and two C sites (Fig. 3, Table 3). The Pb1 and Pb3 atoms are coordinated in one coordination hemisphere by seven O atoms, taking into account strong Pb^{2+}–O bonds shorter than 3.1 Å. In addition, both of the atoms form three long Pb^{2+}–O bonds >3.1 Å each in the opposite coordination hemisphere. This type of coordination geometry of the Pb^{2+} cation can be described as 'hemidirected' (Shimoni-Livny *et al*., 1998). The asymmetric coordination of the Pb1 and Pb3 atoms in $NaPb_5(CO_3)_4(OH)_3$ indicates a strong degree of the stereochemical activity of the $6s^2$ lone pairs of electrons. The coordination sphere of the split Pb2 site (site occupancy factor = ⅙) demonstrates rather uniform distribution of shorter and stronger bonds and can be described as 'holodirected'. 'Holodirected' coordination for Pb^{2+} cations is much less preferable than 'hemidirected' (with shorter and stronger Pb–O bonds concentrated in one coordination hemisphere) in oxysalt compounds.

The splitting of the Pb2 site makes bond-valence analysis of the structure of $NaPb_5(CO_3)_4(OH)_3$ non-applicable. Identical positional disorder for the Pb2 site was observed in the structure of the synthetic analogue of hydrocerussite: $Pb_3(OH)_2(CO_3)_2$

https://doi.org/10.1180/minmag.2017.081.058 Published online by Cambridge University Press

TABLE 2. Crystallographic data and structure-refinement details for $NaPb_5(CO_3)_4(OH)_3$ from Lavrion.

Crystal data	
Formula	$(Na_{0.51}Ca_{0.49})Pb_5(OH)_{2.51}O_{0.49}(CO_3)_4$
Crystal system	hexagonal
Space group	$P6_3/mmc$
Unit-cell dimensions	
a (Å), c (Å)	5.2533(11), 29.425(6)
Unit-cell volume (Å^3)	703.3(3)
Z	2
Calculated density (g·cm^{-3})	6.413
Absorption coefficient (mm^{-1})	59.929
Crystal size (mm)	0.11 × 0.12 × 0.005
Data collection	
Temperature (K)	150(2)
Radiation, wavelength (Å)	Mo$K\alpha$, 0.71073
F(000)	1144
θ range (°)	1.38–27.99
h, k, l ranges	$-6 \le h \le 3$, $-3 \le k \le 6$, $-38 \le l \le 36$
Total reflections collected	7062
Unique reflections (R_{int})	372 (0.03)
Unique reflections $F > 4\sigma(F)$	363
Structure refinement	
Refinement method	Full-matrix least-squares on F^2
Weighting coefficients a, b*	0.03870, 14.70260
Data/restraints/parameters	372/40/12
R_1 [$F > 4\sigma(F)$], wR_2 [$F > 4\sigma(F)$]	0.0470, 0.1412
R_2 all, wR_2 all	0.0475, 0.1417
Goof on F^2	0.990
Largest diff. peak and hole (e·Å^{-3})	4.76 (0.82 Å from Pb1), –2.72 (0.01 Å from Na)

(Martinetto *et al*., 2002) determined by powder XRD utilizing synchrotron radiation. It is also identical to the Pb2 site in the hydrocerussite from Merehead quarry, England (Siidra *et al*., 2018*a*).

One symmetrically independent Na site is coordinated by six O atoms thus forming a trigonal prism. Ca^{2+} detected by the electron microprobe analysis (see above) substitutes Na^+ in the Na site. Occupancy of Na site (Table 3) was fixed in agreement with microprobe data on the last stages of refinement. In order to maintain charge balance, substitution of Na^+ for Ca^{2+} requires some compensation, which we hypothesize to be $OH^- \rightarrow O^{2-}$ on the OH2 site. A similar charge balance mechanism was described recently in the crystal structure of grootfonteinite $Pb_3O(CO_3)_2$ (Siidra *et al*., 2018*b*). The NaO_6 coordination polyhedron contains six equal Na–O bonds of 2.450(14) Å each. The coordination of (Na,Ca) in $NaPb_5(CO_3)_4(OH)_3$ is typical. In general, coordination polyhedron of the Na site is similar to Pb2 (Fig. 3), ignoring the split of the latter. However, the Pb2–OH1 bonds (Table 4) in the equatorial plane of the coordination sphere must be taken into account for bond-valence calculation in $NaPb_5(CO_3)_4(OH)_3$, whereas the Na–OH2 distances (3.033(6) Å × 3 with 0.03 vu each) can be ignored, as they do not contribute significantly to the charge saturation of the Na^+ cations.

The carbonate triangles are very similar and show typical bond lengths, with a <C–O> of 1.277(13) and 1.274(13) Å for C1- and C2-centred triangles, respectively.

Coordination of OH1 and OH2 sites attributed to hydroxyl groups is different. The OH1 site forms one short OH1–Pb1 bond (0.62 vu) and three weaker OH1–Pb2 bonds. In contrast, two short and strong OH2–Pb3 bonds (0.66 vu each) are formed for the OH2 site (Fig. 3). Coordination of the OH1 site is identical to ones in hydrocerussite from Merehead quarry and the powder synthetic analogue of this mineral reported in Martinetto *et al*. (2002), whereas coordination environments of OH2 are similar in abellaite $NaPb_2(CO_3)_2(OH)$ (Krivovichev and Burns, 2000; Belokoneva *et al*., 2002; Ibáñez-Insa *et al*., 2017; Siidra *et al*., 2018*b*). Note, the OH1 site demonstrates additional static disorder in the synthetic analogue of hydrocerussite $Pb_3(OH)_2(CO_3)_2$ (Martinetto *et al*., 2002), whereas our data do not reveal this phenomenon in $NaPb_5(CO_3)_4(OH)_3$.

Structure description

PbO_n (with Pb–O bonds < 3.1 Å) and NaO_6 polyhedra share common oxygen atoms with CO_3 triangles thus forming two types of the two-dimensional (2*D*) blocks shown in Fig. 4. The first block is formed by Pb1, Pb2, C1, O1 and OH1 atoms, whereas Pb3, Na, C2, O2 and OH2 atoms build the second block (Table 3). Notionally, these blocks can be decomposed into three separate

https://doi.org/10.1180/minmag.2017.081.058 Published online by Cambridge University Press

TABLE 3. Atomic coordinates and displacement parameters (Å^2) for $NaPb_5(CO_3)_4(OH)_3$ from Lavrion.

Site	*x/a*	*y/b*	*z/c*	U_{eq}	U^{11}	U^{22}	U^{33}	U^{23}	U^{13}	U^{12}
Hydrocerussite block $[Pb_3(OH)_2(CO_3)_2]^0$										
Pb1	⅓	−⅓	0.09508(4)	0.0182(5)	0.0178(6)	0.0178(6)	0.0190(8)	0	0	0.0089(3)
Pb2*	0.0841(4)	−0.0841(4)	0.00087(16)	0.0250(13)	0.033(2)	0.033(2)	0.0212(19)	−0.0014(10)	0.0014(10)	0.0252(18)
O1	0.386(3)	0.1931(13)	0.0822(4)	0.018(3)	0.004(5)	0.018(5)	0.029(6)	−0.001(2)	−0.001(5)	0.002(3)
OH1	⅓	−⅓	0.0172(9)	0.032(6)	0.037(9)	0.037(9)	0.024(14)	0	0	0.018(5)
C1	⅔	⅓	0.0819(12)	0.018(6)	0.019(10)	0.019(10)	0.016(14)	0	0	0.009(5)
Abellaite block $[NaPb_2(OH)(CO_3)_2]^0$										
Pb3	0	0	0.17308(4)	0.0186(5)	0.0212(5)	0.0212(5)	0.0132(8)	0	0	0.0106(3)
Na**	⅓	⅔	¼	0.0269(12)	0.0270(12)	0.0270(12)	0.0268(17)	0	0	0.0135(6)
OH2***	0	0	¼	0.0574(14)	0.0575(13)	0.0575(13)	0.0574(18)	0	0	0.0287(6)
O2	0.5265(13)	0.053(3)	0.1916(5)	0.020(3)	0.020(5)	0.004(6)	0.031(7)	0.003(5)	0.002(2)	0.002(3)
C2	⅔	⅓	0.1888(15)	0.024(7)	0.012(9)	0.012(9)	0.05(2)	0	0	0.006(4)

*Site occupancy factor = ⅙; ** $Na_{0.51}Ca_{0.49}$; ***$(OH)_{0.51}O_{0.49}$.

sheets (Fig. 5). The two outside sheets in every block contain the Pb atoms and CO_3 groups in a 1:1 ratio and are fully ordered thus giving electroneutral $[PbCO_3]^0$. Each $[PbCO_3]^0$ sheet consists of Pb^{2+} cations, coordinated by three CO_3 triangles each, to form an infinite two-dimensional 'trigonal' mesh pattern perpendicular to the *c* axis. For the sake of discussion these sheets will be given the generic designation *C*, whereby the symbol refers to cerussite, $PbCO_3$, in the crystal structure of which such sheets occur. Two symmetrically independent *C1* and *C2* sheets are formed in the structure of $NaPb_2(CO_3)_2(OH)$. The stereochemically active lone electron pairs on Pb^{2+} cations of Pb1 and Pb3 sites point to each other (Fig. 4). The lone electron pairs on the cations behave as soft ligands that associate together in the interblock space. Sheets of composition $[Pb(OH)_2]^0$ formed by the Pb2 and OH1 sites are sandwiched between the first pair of *C*-type sheets. We denote these sheets as *LHO* (*LHO* = lead hydroxide, according to the $Pb(OH)_2$ composition). Adjacent *C1* sheets of the ⋯*C1*–*LHO*–*C1**⋯ block are related by inversion, and this relationship is indicated by a star symbol: *C1* → *C1** (Figs 4, 5). The resulting $[Pb_3(OH)_2(CO_3)_2]^0$ block with the positional disorder of Pb atoms in the *LHO* sheet is identical to the one in the structure of hydrocerussite $Pb_3(OH)_2(CO_3)_2$.

Similarly the $[Na(OH)]^0$ sheet (*SHO* = sodium hydroxide, according to the approximate Na(OH) composition) is sandwiched between the other two $[PbCO_3]^0$ sheets (*C*2) thus forming the $[NaPb_2(OH)(CO_3)_2]^0$ block described previously in the structure of abellaite $NaPb_2(OH)(CO_3)_2$ (Ibáñez-Insa *et al.*, 2017). The full structural formula of this 2*D* block can be written as $\{[Pb(CO_3)][(Na_{0.51}Ca_{0.49})((OH)_{0.51}O_{0.49})][Pb(CO_3)]\}^0$. As mentioned before, the presence of minor O in the OH2 site plays the role of a charge-compensating agent for the partial substitution of Na^+ by Ca^{2+}. The stacking of the sheets in abellaite-type block can be also symbolized as ⋯*–C2–SHO–C2'*–⋯, whereby the primed symbol indicates that the *C* sheets within a given ⋯*C2–SHO–C2'*⋯ block are related by reflection across a plane perpendicular to [001].

Analysis of the crystal structures of abellaite, hydrocerussite and grootfonteinite $Pb_3O(CO_3)_2$ (Siidra *et al.*, 2018*b*) (Table 5) allows us to suggest that positional disorder of the cations between $[PbCO_3]^0$ sheets occurs when Pb^{2+} is intruded (i.e. in hydrocerussite and grootfonteinite), and is absent in the case of the smaller cation Na^+ (in abellaite).

Thus the structure of the slag phase from the Lavrion is built from alternating $[NaPb_2(OH)$

https://doi.org/10.1180/minmag.2017.081.058 Published online by Cambridge University Press

TABLE 4. Selected interatomic distances in the crystal structure of $NaPb_5(CO_3)_4(OH)_3$ from Lavrion.

Hydrocerussite block $[Pb_3(OH)_2(CO_3)_2]^0$		Abellaite block $[NaPb_2(OH)(CO_3)_2]^0$	
Pb1–OH1	2.29(3)	Pb3–OH2	2.2633(13)
Pb1–O1	2.665(2) × 6	Pb3–O2	2.693(3) × 6
Pb2–Pb2	0.767(4) × 2	Na–O2	2.459(12) × 6
Pb2–Pb2	1.326(7) × 2		
Pb2–Pb2	1.532(8)	C2–O2	1.278(12) × 3
Pb2–OH1	2.318(7)		
Pb2–O1	2.638(14)		
Pb2–OH1	2.783(6) × 2		
Pb2–O1	2.838(13) × 2		
C1–O1	1.276(12) × 3		

$(CO_3)_2]^0$ and $[Pb_3(OH)_2(CO_3)_2]^0$ blocks. There are two blocks (Fig. 4) of each type per unit cell, which corresponds to the following formula: $[Pb_3(OH)_2(CO_3)_2][NaPb_2(OH)(CO_3)_2]$ or $NaPb_5(CO_3)_4(OH)_3$ in simplified form.

Discussion

The structural study demonstrated that at least a part of the well-known presumed 'hydrocerussite' from the Lavrion slags is a different phase formed by both the abellaite- and hydrocerussite-type blocks. This phase is not related directly to plumbonacrite as was suggested by Kolitsch *et al.* (2014). Its structure type is novel for both minerals and synthetic compounds. The structure studied of $NaPb_5(CO_3)_4(OH)_3$ is rather two dimensional and the cohesion of the framework is insured by the weak Pb–O bonds only. The two-dimensional layered structure of $NaPb_5(CO_3)_4(OH)_3$ is clearly

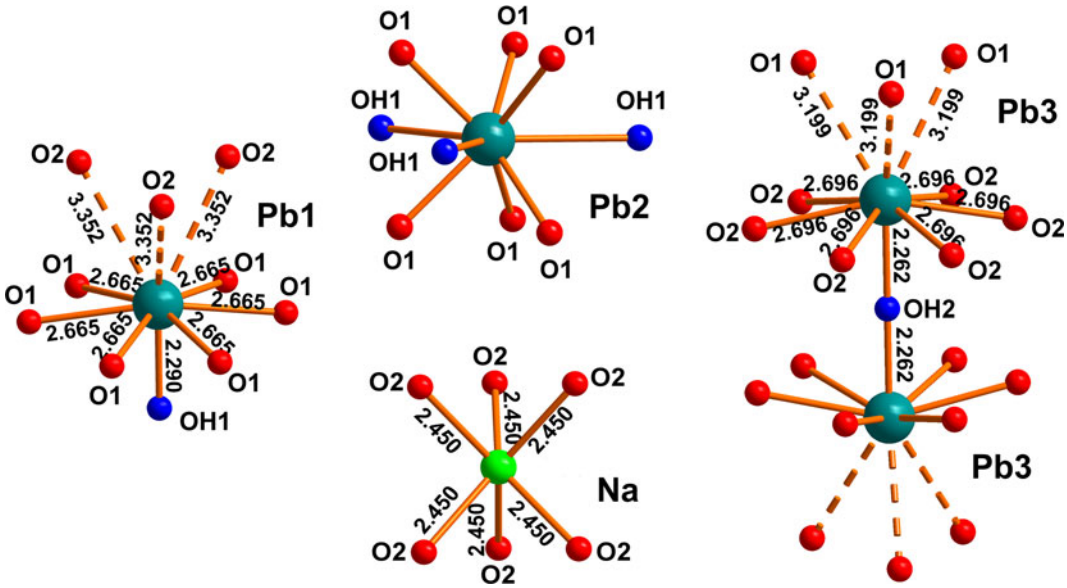

FIG. 3. Cation site coordination environments in the structure of $NaPb_5(CO_3)_4(OH)_3$. The split Pb2 site is represented as fully ordered for clarity and bond distances are not shown.

https://doi.org/10.1180/minmag.2017.081.058 Published online by Cambridge University Press

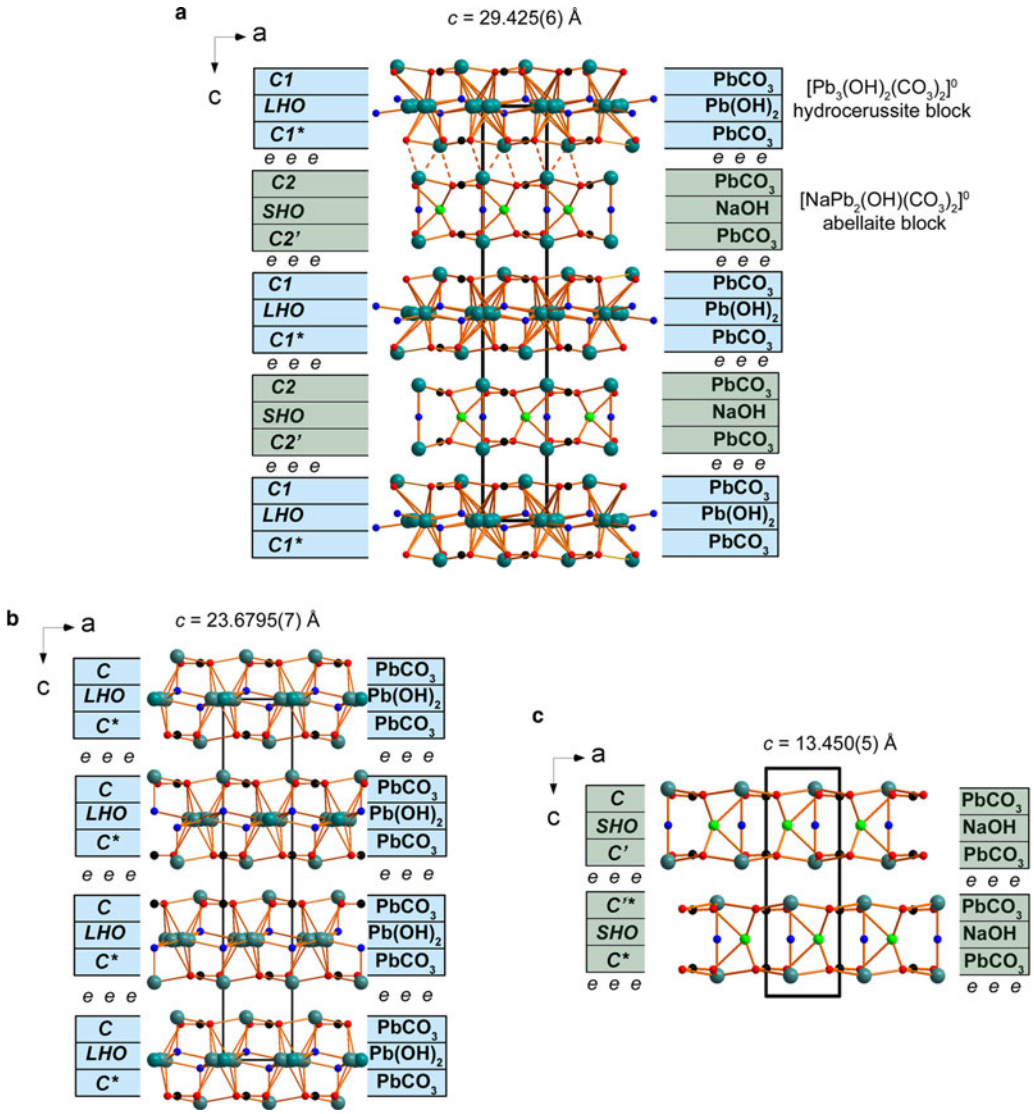

FIG. 4. General projections of the crystal structures of (*a*) $NaPb_5(CO_3)_4(OH)_3$ from Lavrion (weak Pb–O bonds are shown by dashed lines), (*b*) hydrocerussite from Merehead (Siidra *et al.*, 2018*a*) and (*c*) abellaite (Ibáñez-Insa *et al.*, 2017) (modified and drawn for the structure in $P6_3/mmc$). The *c* parameter values are highlighted for each structure. The crystal structure of $NaPb_5(CO_3)_4(OH)_3$ is based on 2*D* blocks very similar to ones in hydrocerussite, $[Pb_3(OH)_2(CO_3)_2]^0$ (blue) and abellaite, $[NaPb_2(OH)(CO_3)_2]^0$ (green). Lone electron pairs on Pb^{2+} cations are symbolized by *e* in between the blocks in the structure of $NaPb_5(CO_3)_4(OH)_3$, hydrocerussite and abellaite. See the text for details.

reflected in the lamellar habit of its crystals and perfect cleavage. This feature is characteristic for other lead hydroxycarbonate minerals including hydrocerussite $Pb_3(OH)_2(CO_3)_2$ (Martinetto *et al.*, 2002; Siidra *et al.*, 2018*a*), plumbonacrite $Pb_5O(OH)_2(CO_3)_3$ (Rumsey *et al.*, 2012), abellaite $NaPb_2(OH)(CO_3)_2$ (Ibáñez-Insa *et al.*, 2017), grootfonteinite $Pb_3O(CO_3)_2$ (Siidra *et al.*, 2018*b*) and leadhillite polymorphs $Pb_4(SO_4)(CO_3)_2(OH)_2$ (Giuseppetti *et al.*, 1990; Steele *et al.*, 1998; Steele *et al.*, 1999). Electroneutral 2*D* blocks of only one topology per structure are observed in the structures

https://doi.org/10.1180/minmag.2017.081.058 Published online by Cambridge University Press

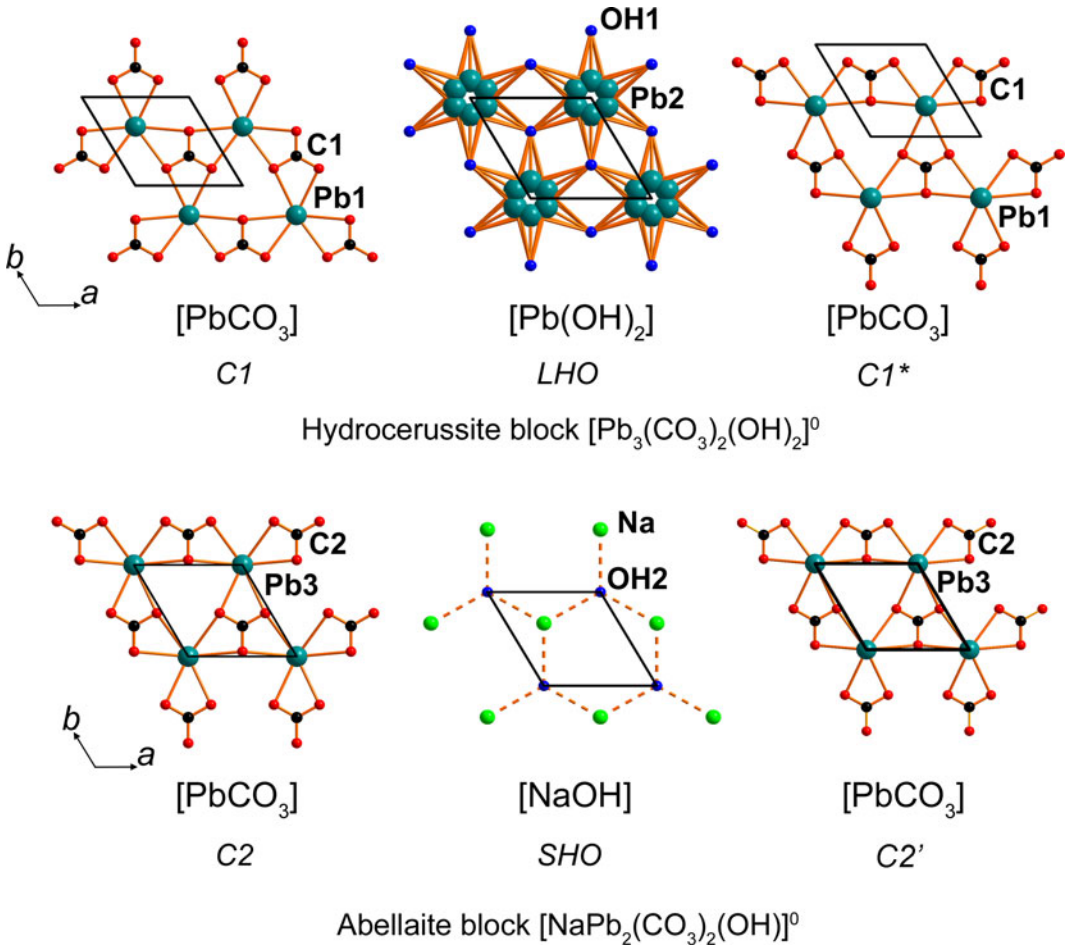

FIG. 5. $[PbCO_3]$ (denoted *C1*), $[Pb(OH)_2]$ (denoted *LHO*) and $[PbCO_3]$ (denoted *C1**) sheets in a hydrocerussite block (above) and $[PbCO_3]$ (denoted *C2*), [NaOH] (denoted *SHO*) and $[PbCO_3]$ (denoted *C2'*) sheets in an abellaite block (below) in the structure of $NaPb_5(CO_3)_4(OH)_3$. See the text for details.

of all these minerals. The crystal structure of $NaPb_5(CO_3)_4(OH)_3$ is unique for lead hydroxy-carbonates and, moreover, exclusive for layered minerals in general, as it demonstrates interstratification of neutral blocks of minerals significantly different in chemical composition and topology. However, the structural architecture of $[Pb_3(OH)_2(CO_3)_2][NaPb_2(OH)(CO_3)_2] = NaPb_5(CO_3)_4(OH)_3$ resembles the organization of the crystal structure of $[Tl_5^+(SiO_4)(OH)]_2[Tl_6^+(SO_4)(OH)_4] = Tl_{16}^+(SiO_4)_2(SO_4)(OH)_6$ (Siidra *et al.*, 2014). Note, stereochemically active $6s^2$ lone electron pairs on Pb^{2+} or Tl^+ cations play an important role for the formation of such structural architectures and may result in the very different stackings of 2*D* blocks.

The formation of $NaPb_5(CO_3)_4(OH)_3$, as well as the previously known abellaite-type phase $NaPb_2(OH)(CO_3)_2$ in Lavrion slags, is caused by the contact of lead slags with the seawater over the last several thousand years. However the recent find of abellaite (Ibáñez-Insa *et al.*, 2017) in the Eureka mine, Catalonia, Spain, indicates the possibility of its formation under different conditions. Hydrocerussite itself is a stable mineral under different environmental conditions with high pH values. Thus we hypothesize that the $NaPb_5(CO_3)_4(OH)_3$ phase may exist as a mineral at some exotic conditions. Recently we have described grootfonteinite $Pb_3O(CO_3)_2$ (Siidra *et al.*, 2018*b*) from the Kombat mine, Namibia. The topology of 2*D* blocks in the crystal

https://doi.org/10.1180/minmag.2017.081.058 Published online by Cambridge University Press

TABLE 5. Comparative data of $NaPb_5(CO_3)_4(OH)_3$, hydrocerussite and abellaite.

Mineral/compound	Unnamed phase from Lavrion	Hydrocerussite	Abellaite
Formula	$NaPb_5(CO_3)_4(OH)_3$	$Pb_3(OH)_2(CO_3)_2$	$NaPb_2(OH)(CO_3)_2$
Crystal system	Hexagonal	Trigonal	Hexagonal
Space group	$P6_3/mmc$	$R\bar{3}m$*	$P6_3mc$***
a (Å)	5.2533(11)	5.2475(1)	5.254(2)
c (Å)	29.425(6)	23.6795(7)	13.450(5)
V (Å^3)	703.3(3)	564.69(1)	321.5(2)
R_1 (%)	4.70	2.10	–
Strongest lines of the powder XRD pattern: d, Å (I, %)	4.126 (29)	4.470 (33)	3.193 (100)
	3.336 (100)	4.237 (32)	2.627 (84)
	3.088 (18)	3.601 (63)	2.275 (29)
	2.626 (30)	3.279 (100)	2.243 (65)
	2.454 (17)	2.632 (88)	2.029 (95)
	2.063 (20)	2.230 (23)	2.011 (25)
D (g cm^{-3})	6.41 (calc.)	6.80–6.82 (meas.)** 6.84 (calc.)*	5.90 (calc.)
Sources	This work	*Siidra *et al*. (2018*a*) **Palache *et al*. (1951); Anthony *et al*. (2003)	Ibáñez-Insa *et al*. (2017)

*Hydrocerussite from the Merehead quarry, Somerset, England; **Palache *et al*. (1951) and Anthony *et al*. (2003) do not provide structural data; *** powder XRD data were indexed in Ibáñez-Insa *et al*. (2017) after the structural data provided in Krivovichev and Burns (2000); the correct space group is most likely $P6_3/mmc$ (Siidra *et al*., 2018*b*).

structure of grootfonteinite can be considered as intermediate between those of abellaite and hydrocerussite. Further, new lead hydroxycarbonate minerals with structural architectures organized *via* similar building principles (i.e. based on 2*D* blocks of different composition and topology) as in $NaPb_5(CO_3)_4(OH)_3$ are anticipated.

Acknowledgements

The authors are grateful to Peter Leverett, Gerald Giester and Daniel Atencio for valuable comments. This work was supported by St. Petersburg State University through the internal grant 3.38.238.2015 and 3.42.1495.2015 (for part of the XRD and crystal-structure studies) and by the Russian Science Foundation, grant no. 14-17-00048 (for part of the electron probe and IR spectroscopy studies). Technical support by the X-Ray Diffraction Resource Centre of Saint-Petersburg State University is gratefully acknowledged.

Supplementary material

To view supplementary material for this article, please visit https://doi.org//10.1180/minmag.2017.081.058.

References

Anthony, J.W., Bideaux, R.A., Bladh, K.W. and Nichols, M. C. (2003) *Handbook of Mineralogy. V. Borates, Carbonates, Sulfates*. Mineral Data Publishing, Tucson.

Belokoneva, E.L., Al'-Ama, A.G., Dimitrova, O.V., Kurazhkovskaya, V.S. and Stefanovich, S.Yu. (2002) Synthesis and crystal structure of new carbonate $NaPb_2(CO_3)_2(OH)$. *Crystallography Reports*, **47**, 217–222.

Gelaude, P., van Kalmthout, P. and Rewitzer, C. (1996) *Laurion: The Minerals in the Ancient Slags*. Janssen Print, Nijmegen, The Netherlands.

Giuseppetti, G., Mazzi, F. and Tadini, C. (1990) The crystal structure of leadhillite: $Pb_4(SO_4)(CO_3)_2(OH)_2$. *Neues Jahrbuch für Mineralogie Monatshefte*, **1990**, 255–268.

Ibáñez-Insa, J., Elvira, J.J., Llovet, X., Pérez-Cano, J., Oriols, N., Busquets-Masó, M. and Hernández, S. (2017) Abellaite, $NaPb_2(CO_3)_2(OH)$, a new supergene mineral from the Eureka mine, Lleida province, Catalonia, Spain. *European Journal of Mineralogy*, **29**, 915–922.

Kokkoros, P. and Vassiliadis, K. (1953) Röntgenkristallographie von Hydrocerussit. *Tschermaks Mineralogische und Petrographische Mitteilungen*, **3**, 298–304.

https://doi.org/10.1180/minmag.2017.081.058 Published online by Cambridge University Press

Kolitsch, U., Rieck, B., Brandstätter, F., Schreiber, F., Fabritz, K. H., Blaß, G. and Gröbner, J. (2014) Neufunde aus dem altem Bergbau und den Schlacken von Lavrion (II). *Mineralien-Welt*, **25**, 82–95.

Krivovichev, S.V. and Burns, P.C. (2000) Crystal chemistry of basic lead carbonates. III. Crystal structures of $Pb_3O_2(CO_3)$ and $NaPb_2(CO_3)_2(OH)$. *Mineralogical Magazine*, **64**, 1077–1087.

le Page, Y. (1987) Computer derivation of the symmetry elements implied in a structure description. *Journal of Applied Crystallography*, **20**, 264–269.

Libowitzky, E. (1999) Correlation of O–H stretching frequencies and O–H···O hydrogen bond lengths in minerals. *Monatshefte für Chemie*, **130**, 1047–1059.

Martinetto, P., Anne, M., Dooryhée, E., Walter, P. and Tsoucaris, G. (2002), Synthetic hydrocerussite, $2PbCO_3{\cdot}Pb(OH)_2$, by X-ray powder diffraction. *Acta Crystallographica*, **C58**, i82–i84.

Nickel, E.H. and Grice, J.D. (1998) The IMA Commission on New Minerals and Mineral Names: procedures and guidelines on mineral nomenclature, 1998. *Mineralogy and Petrology*, **64**, 237–263.

Palache, C., Berman, H. and Frondel, C. (1951) *Dana's System of Mineralogy (7th edition), vol. II*. John Wiley, New York.

Rumsey, M.S., Siidra, O.I., Krivovichev, S.V., Spratt, J., Stanley, C.J. and Turner, R.W. *IMA* 11-*G: Plumbonacrite is revalidated*. CNMNC Newsletter No. 14, October 2012, page 1288; *Mineralogical Magazine*, **76**, 1281–1288.

Sheldrick, G.M. (2015) New features added to the refinement program SHELXL since 2008 are described and explained. *Acta Crystallographica*, **C71**, 3–8.

Shimoni-Livny, L., Glusker, J.P. and Bock, C.W. (1998) Lone pair functionality in divalent lead compounds. *Inorganic Chemistry*, **37**, 1853–1867.

Spek, A.L. (2003) Single-crystal structure validation with the program PLATON. *Journal of Applied Crystallography*, **36**, 7–13.

Siidra, O.I., Britvin, S.N., Krivovichev, S.V., Klimov, D. A. and Depmeier, W. (2014) Crystallography between Kiel and St. Petersburg: review of collaboration and the crystal structure of $[Tl_5(SiO_4)(OH)]_2[Tl_6(SO_4)(OH)_4]$. *Zeitschrift für Kristallographie – Crystalline Materials*, **229**, 753–759.

Siidra, O.I., Nekrasova, D.O., Depmeier, W., Chukanov, N. V., Zaitsev, A.N. and Turner, R. (2018*a*) Hydrocerussite-related minerals and materials: structural principles, chemical variations and infrared spectroscopy. *Acta Crystallographica*, **B74**, 182–195.

Siidra, O.I., Jonsson, E., Chukanov, N.V., Nekrasova, D. O., Pekov, I.V., Depmeier, W., Polekhovsky, Yu. S. and Yapaskurt, V.O. (2018*b*) Grootfonteinite, $Pb_3O(CO_3)_2$, a new mineral species from the Kombat mine, Namibia, merotypically related to hydrocerussite. *European Journal of Mineralogy*, https://doi.org/10.1127/ejm/2018/0030-2723

Steele, I.M., Pluth, J.J. and Livingstone, A. (1998) Crystal structure of macphersonite $Pb_4SO_4(CO_3)_2(OH)_2$ comparison with leadhillite. *Mineralogical Magazine*, **62**, 451–459.

Steele, I.M., Pluth, J.J. and Livingstone, A. (1999) Crystal structure of susannite, $Pb_4SO_4(CO_3)_2(OH)_2$: a trimorph with macphersonite and leadhillite. *European Journal of Mineralogy*, **11**, 493–499.

https://doi.org/10.1180/minmag.2017.081.058 Published online by Cambridge University Press